J|A|C|S ARTICLES

Published on Web 07/06/2009

Green Electrogenerated Chemiluminescence of Highly Fluorescent Benzothiadiazole and Fluorene Derivatives

Khalid M. Omer,[†] Sung-Yu Ku,[‡] Ken-Tsung Wong,*[,‡] and Allen J. Bard*[,†]

Center for Electrochemistry and Department of Chemistry and Biochemistry, The University of Texas at Austin, Austin, Texas 78712, and Department of Chemistry, National Taiwan University, 106 Taipei, Taiwan

Received May 21, 2009; E-mail: ajbard@mail.utexas.edu; kenwong@ntu.edu.tw

Abstract: A group of highly fluorescent 2,1,3-benzothiadiazole derivatives (**BH0**−**BH3**), including two fluorene derivatives (**AB2** and **C01**) were synthesized and characterized. The electrochemical, spectroscopic, and electrogenerated chemiluminescence (ECL) properties of the compounds were determined. Benzothiadiazole derivatives **BH1**, **BH2**, and **BH3** show reversible oxidation and reduction waves and produce strong green ECL in nonaqueous solutions. This ECL could be seen by the naked eye, even in a well lit room. The fluorene derivatives, **C01** and **AB2**, also produce bright, easily observable ECL. Since the ECL spectra are at essentially the same wavelengths as the photoluminescence (PL) spectra, and the energies of the electron transfer reactions are greater than the singlet state energies, we propose direct formation of the excited singlet state during ion annihilation. **BH0**, which shows a quasi-reversible oxidation wave, only produced weak ECL via direct annihilation but gave strong ECL with benzoyl peroxide (BPO) as a coreactant. The ECL quantum efficiencies of the series, compared to that of 9,10-diphenylanthrace, was estimated to range from 0.05 to 7%. This series shows rare green photoluminescence (λ_{PL} = 490−556 nm) with a high PL quantum efficiency in solution (Φ = 5 to 90%).

Introduction

In this work, we report the synthesis, electrochemical, and photophysical characterization, as well as the electrogenerated chemiluminescence (ECL) of a series of novel, low-molecular weight, highly fluorescent 2,1,3-benzothiadiazole derivatives (Scheme 1). ECL is a unique type of luminescence in which the electron transfer between electrogenerated ion radicals produces an electronically excited product in the vicinity of the electrode, with the emission of light.[1]

As shown here and in previous publications, ECL and electrochemistry are versatile and sensitive tools that can be used to obtain valuable information about radical ion formation and stability and about often subtle interactions within molecules. Such information is of use in the design of organic light emitting devices (OLEDs), where charge creation, migration, and recombination are determined by analogous charged states in the active organic layer.[2] Another use of ECL involves development of new ECL emitters for labels at different wavelengths for bioanalytical applications, i.e., finding ECL emitters of wavelengths different from the currently used species.

Fluorene-based materials, such as terfluorenes,[3] oligofluorene,[4] and polyfluorenes,[5] have emerged as promising candidates for OLEDs due to their high photoluminescence (PL) and electroluminescence (EL) efficiencies, good thermal stability, and color tunability across the full visible range. Tuning of the emission can be achieved by adding more units of conjugation or modulation of the donor and acceptor strength in bipolar compounds.[6] Generally, fluorene derivatives emit blue light due to their large energy gap. By introducing a unit with a narrower energy gap, like the electron-deficient 2,1,3-benzothiadiazole group into the fluorene backbone, the emission color can be

[†] The University of Texas at Austin.
[‡] National Taiwan University.

(1) For review on ECL, see: (a) *Electrogenerated Chemiluminescence*; Bard, A. J.; Ed.; Marcel Dekker, Inc.: New York, 2004. (b) Miao, W. *Chem. Rev.* **2008**, *108*, 2506. (c) Richter, M. M. *Chem. Rev.* **2004**, *104*, 3003. (d) Knight, A. W.; Greenway, G. M. *Analyst* **1994**, *119*, 879. (e) Bard, A. J.; Debad, J. D.; Leland, J. K.; Sigal, G. B.; Wilbur, J. L.; Wohlstadter, J. N. In *Encyclopedia of Analytical Chemistry: Applications, Theory and Instrumentation*; Meyers, R. A., Ed.; John Wiley & Sons: New York, 2000; Vol. 11, p 9842.

(2) Yasuda, T.; Imase, T.; Yamamaoto, T. *Macromolecules* **2005**, *38*, 7378.

(3) (a) Wong, K.-T.; Chien, Y.-Y.; Chen, R.-T.; Wang, C.-F.; Lin, Y.-T.; Chiang, H.-H.; Hsieh, P.-Y.; Wu, C.-C.; Chou, C. H.; Su, Y. O.; Lee, G.-H.; Peng, S.-M. *J. Am. Chem. Soc.* **2002**, *124*, 11576. (b) Wu, F.-I.; Dodda, R.; Reddy, D. S.; Shu, C.-F. *J. Mater. Chem.* **2002**, *12*, 2893. (c) Tsolakis, P. K.; Kallitsis, J. K. *Chem.—Eur. J.* **2003**, *9*, 936. (d) Wu, C.-C.; Lin, Y.-T.; Wong, K.-T.; Chen, R.-T.; Chien, Y.-Y. *Adv. Mater.* **2004**, *16*, 61. (e) Chochos, C. L.; Kallitsis, J. K.; Gregoriou, V. G. *J. Phys. Chem. B* **2005**, *109*, 8755. (f) Chochos, C. L.; Kallitsis, J. K.; Keivanidis, P. E.; Baluschev, S.; Gregoriou, V. G. *J. Phys. Chem. B* **2006**, *110*, 4657. (g) Chen, A. C.-A.; Wallace, J. U.; Klubek, K. P.; Madaras, M. B.; Tang, C. W.; Chen, S. H. *Chem. Mater.* **2007**, *19*, 4043.

(4) (a) Lee, S. H.; Tsutsui, T. *Thin Solid Films* **2000**, *363*, 76. (b) Geng, Y.; Katsis, D.; Culligan, S. W.; Ou, J. J.; Chen, S. H.; Rothberg, L. *J. Chem. Mater.* **2002**, *14*, 463. (c) Li, Y.; Ding, J.; Day, M.; Tao, Y.; Lu, J.; D'iorio, M. *Chem. Mater.* **2003**, *15*, 4936. (d) Culligan, S. W.; Geng, Y.; Chen, S. H.; Klubek, K.; Vaeth, K. M.; Tang, C. W. *Adv. Mater.* **2003**, *15*, 1176. (g) Kanibolotsky, A. L.; Berridge, R.; Skabara, P. J.; Perepichka, I. F.; Bradley, D. D. C.; Koeberg, M. *J. Am. Chem. Soc.* **2004**, *126*, 13695. (h) Liu, Q.-D.; Lu, J.; Ding, J.; Day, M.; Tao, Ye.; Barrios, P.; Stupak, J.; Chan, K.; Li, J.; Chi, Y. *Adv. Funct. Mater.* **2007**, *17*, 1028. (i) Kong, Q.; Zhu, D.; Quan, Y.; Chen, Q.; Ding, J.; Lu, J.; Tao, Y. *Chem. Mater.* **2007**, *19*, 3309.

Scheme 1

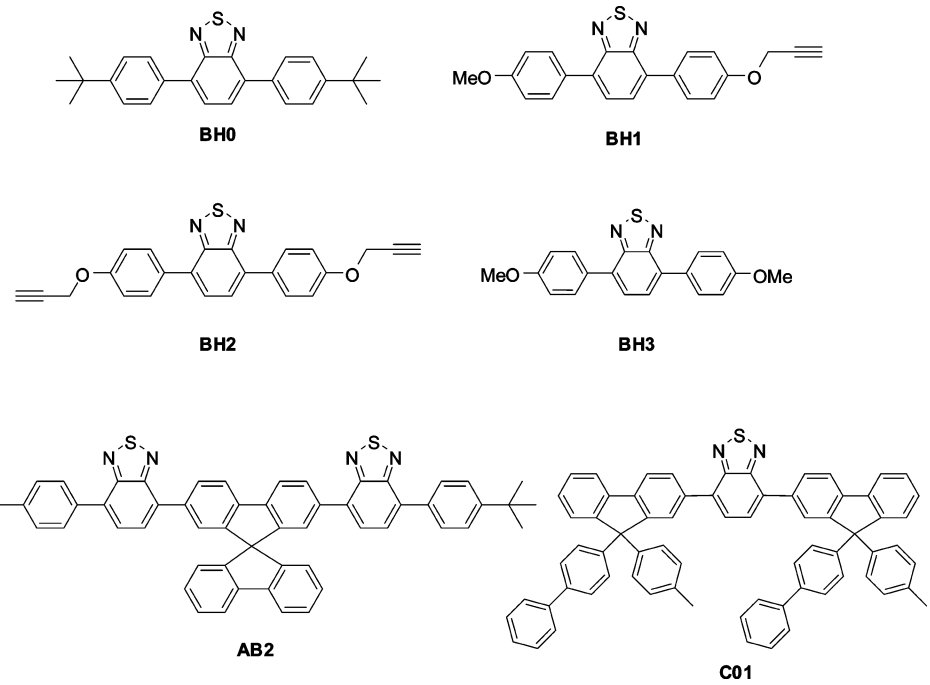

Scheme 2. Synthetic Route for **BH0**

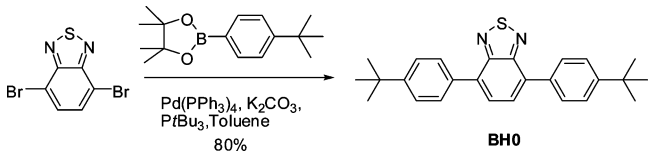

tuned to the green region.[7] Therefore, the ability to tune the luminescence of these systems also makes them of interest for developing new, multicolor, light-emitting materials which are needed for full color displays and also to achieve multiple wavelength ECL labels.

We previously reported the electrochemical behavior and ECL of *ter*-9,9-diarylflourenes,[8] spirobifluorene-bridged bipolar systems with stable radical ions,[9] star-shaped truxene core-oligofluorene,[10] and *N*-phenylcarbazole bridged dispirobifluorene.[11]

ECL involves electron transfer between electrochemically generated species, often radical ions, which results in an excited species that emits light.[1] The simplest ECL process is the radical ion annihilation reaction, which can be represented as follows

$$D + e^- \rightarrow D^{\bullet -} \quad \text{(formation of radical anion)} \qquad (1)$$

$$D - e^- \rightarrow D^{\bullet +} \quad \text{(formation of radical cation)} \qquad (2)$$

$$D^{\bullet -} + D^{\bullet +} \rightarrow {}^1D^* + D \quad \text{(excited state formation)} \qquad (3)$$

$${}^1D^* \rightarrow D + h\nu \quad \text{(ECL emission)} \qquad (4)$$

The energy available for excited state generation is approximately equal to the enthalpy of annihilation: $-\Delta H^o = -\Delta G^o - T\Delta S^o$. If $-\Delta H^o$ is greater than the energy of an excited state, E_s (singlet) or E_T (triplet), a molecule can achieve that state upon radical ion annihilation. If the singlet state is directly populated, then the ECL mechanism is referred to as S-route ECL. If the triplet state is populated, triplet−triplet annihilation can occur to create a singlet state in what is known as T-route ECL.[12,1a]

(5) (a) Chang, S.-C.; Li, Y.; Yang, Y. *J. Phys. Chem. B* **2000**, *104*, 11650. (b) Lupton, J. M.; Craig, M. R.; Meijer, E. W. *Appl. Phys. Lett.* **2002**, *80*, 4489. (c) Wong, K.-T.; Chien, Y.-Y.; Chen, R.-T.; Wang, C.-F.; Lin, Y.-T.; Chiang, H.-H.; Hsieh, P.-Y.; Wu, C.-C.; Chou, C. H.; Su, Y. O.; Lee, G.-H.; Peng, S.-M. *J. Am. Chem. Soc.* **2002**, *124*, 11576. (d) Ego, C.; Grimsdale, A. C.; Uckert, F.; Yu, G.; Srdanov, G.; Mullen, K. *Adv. Mater.* **2002**, *14*, 809. (e) Culligan, S. W.; Geng, Y.; Chen, S. H.; Klubek, K.; Vaeth, K. M.; Tang, C. W. *Adv. Mater.* **2003**, *15*, 1176. (f) Wu, W.; Inbasekaran, M.; Hudack, M.; Welsh, D.; Yu, W.; Cheng, Y.; Wang, C.; Kram, S.; Tacey, M.; Bernius, M.; Fletcher, R.; Kiszka, K.; Munger, S.; O'Brien, J. *Microelectron. J.* **2004**, *35*, 343. (g) Huang, F.; Wu, H.; Wang, D.; Yang, W.; Cao, Y. *Chem. Mater.* **2004**, *16*, 708. (h) Wong, K.-T.; Liao, Y.-L.; Lin, Y.-T.; Su, H.-C.; Wu, C.-C. *Org. Lett.* **2005**, *7*, 5131. (i) Chen, A. C.-A.; Wallace, J. U.; Wei, S. K.-H.; Zeng, L.; Chen, S. H. *Chem. Mater.* **2006**, *18*, 204. (j) Fan, S.; Sun, M.; Wang, J.; Yang, W.; Cao, Y. *Appl. Phys. Lett.* **2007**, *91*, 213502.
(6) (a) Joshi, H. S.; Jamshidi, R.; Tor, Y. *Angew. Chem., Int. Ed.* **1999**, *38*, 2721. (b) Yoshida, Y.; Tanigaki, N.; Yase, K.; Hotta, S. *Adv. Mater.* **2000**, *12*, 1587. (c) Tsuzuki, T.; Shirasawa, N.; Suzuki, T.; Tokito, S. *Adv. Mater.* **2003**, *15*, 1455. (d) Montes, V. A.; Li, G.; Pohl, R.; Shinar, J.; Anzenbacher, P. *Adv. Mater.* **2004**, *16*, 2001. (e) Gana, J.-A.; Song, Q. L.; Hou, X- Y.; Chen, K.; Tian, H. *J. Photochem. Photobiol. A* **2004**, *162*, 399.
(7) (a) Millard, I. S. *Synth. Met.* **2000**, *111*−*112*, 119. (b) Muller, C. D.; Falcou, A.; Reckefuss, N.; Rojahn, M.; Wiederhirn, V.; Rudati, P.; Frohne, H.; Nuyken, O.; Becker, H.; Meerholz, K. *Nature* **2003**, *421*, 829. (c) Justin Thomas, K. R.; Lin, J. T.; Velusamy, M.; Tao, Y.-T.; Chuen, C.-H. *Adv. Funct. Mater.* **2004**, *14*, 83. (d) Lin, J.; Dong, J.; Zhou, Q.; Geng, Y.; Ma, D.; Wang, L.; Jing, X.; Wang, F. *J. Mater. Chem.* **2007**, *17*, 2832.
(8) Choi, J. P.; Wong, K. T.; Chen, Y. M.; Yu, J. K.; Chou, P. T.; Bard, A. J. *J. Phys. Chem. B* **2003**, *107*, 14407.
(9) Fungo, F.; Wong, K.-T.; Ku, S.-Y.; Hung, Y.-Y.; Bard, A. J. *J. Phys. Chem. B* **2005**, *109*, 3984.
(10) Omer, K. M.; Kanibolotsky, A. L.; Skabara, P. J.; Perepichka, I. F.; Bard, A. J. *J. Phys. Chem. B* **2007**, *111*, 6612.
(11) Rashidnadimi, S.; Hung, T.-H.; Wong, K.-T.; Bard, A. J. *J. Am. Chem. Soc.* **2008**, *130*, 634.
(12) (a) Sartin, M. M.; Zhang, H.; Zhang, J.; Zhang, P.; Tian, W.; Wang, Y.; Bard, A. J. *J.Phys. Chem. C* **2007**, *111*, 16350. (b) Lai, R. Y.; Fleming, J. J.; Merner, B. L.; Vermeij, R. J.; Bodwell, G. J.; Bard, A. J. *J. Phys. Chem A* **2004**, *108*, 376.

Scheme 3. Synthetic Routes for **BH1**, **BH2**, and **BH3**

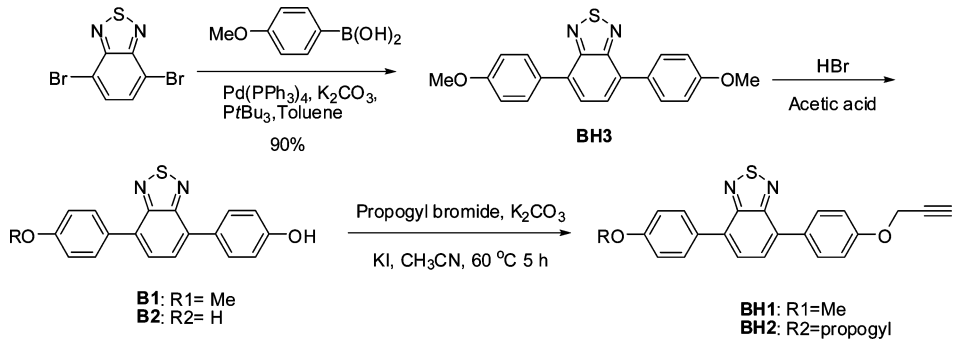

Scheme 4. Synthetic Route of **AB2**

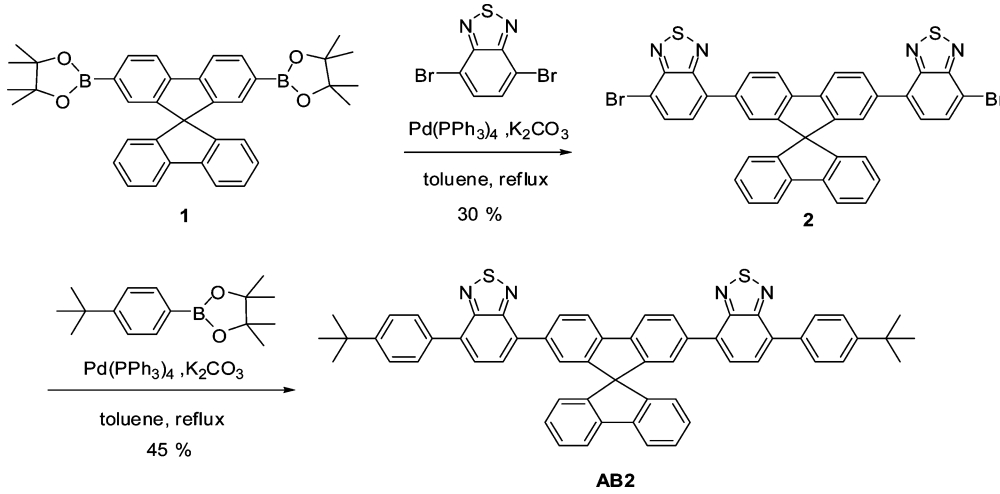

If either the cation radical or anion radical is unstable (e.g., if the radical cation or anion is unstable or cannot be generated prior to the oxidation or reduction of solvent or supporting electrolyte), then ECL can often be generated by use of a coreactant, which can form either a strong reducing agent when oxidized (as oxalate or tripropylamine) or a strong oxidizing agent when reduced (as persulfate or benzoyl peroxide). For example, the oxidation wave of **BH0** is not chemically reversible at scan rates of 100 mV/s (i.e., the cation radical is not stable), so benzoyl peroxide (BPO) was used as a coreactant for ECL studies of this species. BPO forms a strong oxidizing agent (E^{oxd} = +1.5 V vs SCE)[13,1a] and leads to the singlet excited state of **BH0** (D*) as follows

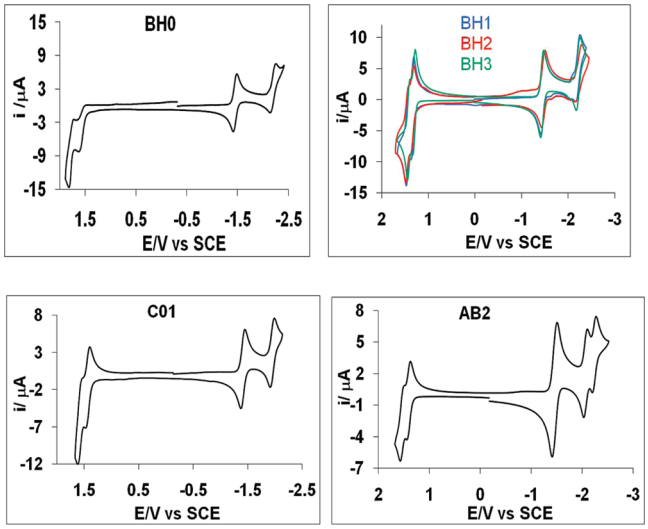

Figure 1. Cyclic voltammograms for the compounds, supporting electrolyte 0.1 M Bu_4NPF_6:1 mM (**BH0**, **BH1**, **BH2**, **BH3**) in MeCN, 1 mM (**C01, AB2**) in 1:1 MeCN:Bz. Scan rate: 100 mV/s, WE:Pt disk electrode (~1 mm diameter), CE:Pt coiled electrode.

$$BPO + e^- \rightarrow BPO^{\bullet -} \quad (5)$$

$$BPO^{\bullet -} \rightarrow BPO^- + BPO^{\bullet} \quad (6)$$

$$BPO^{\bullet} + D^{\bullet -} \rightarrow BPO^- + D^* \quad (7)$$

Here we describe the synthesis, electrochemistry, spectroscopy, and ECL of a series of benzothiadiazole and fluorene derivatives. The electrochemical reduction, oxidation, and radical ion annihilation ECL of the benzothiadiazole derivatives (**BH0**−**BH3**) and fluorene derivatives (**AB2** and **C01**) are described below. Photophysical measurements were carried out, and a comparison of their ECL spectra and PL is discussed.

Synthesis of Benzothiadiazole Derivatives. Details of the synthetic procedures and product characterizations are given in the Supporting Information. Scheme 2 shows the synthesis of **BH0** by Suzuki coupling of dibromobenzothiadiazole with 4-*tert*-butylphenylboronic ester in the presence of a catalytic amount of $Pd(PPh_3)_4$ and P^tBu_3, leading to **BH0** in an isolated yield of 80% after purification through recrystallization.

Table 1. Electrochemical Data

	oxidation waves, V vs SCE		reduction waves, V vs SCE			D ($\times 10^{-6}$)	E_g[b]	E_{HOMO}[c]	$E_{(LUMO)}$[d]
Cpd[a]	$E_{1/2}^{oxd1}$	$E_{1/2}^{oxd2}$	$E_{1/2}^{red1}$	$E_{1/2}^{red2}$	$E_{1/2}^{red3}$	cm^2/s	(eV)	(eV)	(eV)
BH0	1.64(E_p)	1.83(E_p)	−1.40	−2.18	−	9.0	3.04	−6.02	−2.93
BH1	1.37	1.49	−1.40	−2.18	−	9.0	2.77	−5.75	−2.93
BH2	1.42	1.54	−1.38	−2.18	−	9.0	2.80	−5.79	−2.92
BH3	1.33	1.45	−1.42	−2.21	−	9.0	2.75	−5.71	−2.92
C01	1.46	1.61	−1.39	−1.93	−	7.5	2.85	−5.84	−2.89
AB2	1.43	1.56	−1.44	−2.05	−2.20	7.0	2.87	−5.81	−2.88

[a] Concentrations, 1 mM. [b] From the CV. [c] The HOMO values are calculated based on the value of −4.8 eV for ferrocene with respect to the vacuum.[17,9] [d] From the first reduction wave.

Scheme 3 depicts the synthetic routes for **BH1**, **BH2**, and **BH3**.[14] A Suzuki coupling reaction of 4,7-dibromo-2,1,3-benzothiadiazole with 4-methoxyphenylboronic acid in the presence of a catalytic amount of $Pd(PPh_3)_4$ and P^tBu_3 gave **BH3** in an isolated yield of 90% after purification through recrystallization. Subsequent selective monodeprotection or dideprotection of **BH3** afforded **B1** and **B2** by means of excess amounts of HBr (33% in HOAc). Then, treatment of **B1** and **B2** with excess amounts of propagyl bromide, K_2CO_3, and a catalytic amount of KI (10 mol %) in acetonitrile at 60 °C for 5 h led to the desired compound **BH1** and **BH2** in a good yield of 80% and 99%, respectively.

Synthesis of AB2. AB2, which consisted of a spirobifluorene core, benzothiadiazole moieties, and *tert*-butylbenzene, was synthesized from 4,7-dibromo-2,1,3-benzothiadiazole and 9,9′-spirobifluorene 2,7-diboronic ester (**1**) through a Suzuki coupling reaction. Scheme 4 depicts the synthetic route of **AB2** from compound **1**. Selective Suzuki coupling of the diboronate **1** with a large amount (6 equiv) of dibromo-benzothiadiazole afforded the dibromo **2** in 30% yields. Then Suzuki coupling of the dibromo **2** with 4-*tert*-butylphenylboronic ester afforded **AB2** in 45% yield.

C01 was previously used as an efficient green emitter in an organic light-emitting diode.[15]

Experimental Section

Materials. Anhydrous acetonitrile (MeCN, 99.93%, in a sure-sealed bottle) and anhydrous benzene (Bz, 99.8% in a sure-sealed bottle) were obtained from Aldrich. Tetra-*n*-butylammonium hexafluorophosphate (n-Bu_4NPF_6) was used as received from Fluka and benzoyl peroxide (BPO) (reagent grade, 97%) from Aldrich. All solutions were prepared in a glovebox (Vacuum Atmospheres Corp.) and placed in airtight vessels for electrochemical and ECL measurements outside of the glovebox.

Characterization. The electrochemical cell consisted of a working electrode with a ∼1 mm diameter inlaid platinum disk, a Ag wire quasireference electrode (referenced after each series of experiments against the ferrocene/ferrocenium couple to obtain the potentials vs SCE), and a Pt wire counter electrode. For ECL, the working electrode was a 2 mm inlaid J-type (bent to face the detector) platinum disk. The working electrode was polished with 1 μm alumina (Buehler, Ltd., IL), then 0.3 μm, and 0.05 μm, followed by sonication in DI water and ethanol for 5 min each.

Cyclic voltammograms (CVs) were recorded on a model 660 electrochemical workstation (CH Instruments, Austin, TX). Faradaic current and ECL transients were simultaneously recorded using an Autolab electrochemical workstation (Eco Chemie, The Netherlands) coupled with a photomultiplier tube (PMT, Hammamatsu R4220p, Japan) held at −750 V with a high-voltage power supply (Kepco, Flushing, NY). The photocurrent produced at the PMT was converted to a voltage signal with an electrometer/high resistance system (Keithley, Cleveland, OH) and fed into the external input channel of an analog-to-digital converter (ADC) of the Autolab. The ECL spectra were taken using a calibrated charge coupled device (CCD) camera (Princeton Instruments, SPEC-32). Absorption spectra were recorded with a Milton Roy Spectronic 3000 array spectrophotometer. Fluorescence spectra were acquired on a QuantaMaster spectrofluorimeter (Photon Technology International, Birmingham, NJ). DigiSim 3.03 (Bioanalytical Systems, Inc., West Lafayette, IN) was used to simulate the cyclic voltammograms.

Electrochemistry. Oxidation and reduction potentials provide information concerning the relative energetic positions of the frontier orbitals. Cyclic voltammetry was used to probe the electrochemistry of the compounds, assess the stability of the radical ions in the solution, and find the energy of the radical ion annihilation in ECL. CVs of these compounds are shown in Figure 1, and the electrochemical results are summarized in Table 1.

Benzothiadiazole Derivatives (BH0, BH1, BH2, and BH3). Oxidation. These four compounds differ only in the substituents on each phenyl and generally show similar behavior. The electrochemical results are summarized in Table 1. Upon scanning to positive potentials, all show two consecutive, closely spaced, one-electron transfer peaks. These peaks correspond to the formation of the radical cation and dication since the consecutive peaks have similar peak currents, ∼5 μA. The first oxidation waves for **BH1**, **BH2**, and **BH3** were chemically reversible at scan rates as low as 50 mV/s, showing that the radical cations were stable in the time scale of the experiment. The peak separation for reversible oxidation peaks was ∼70 mV, slightly larger than the expected value for nernstian behavior for a one-electron transfer reversible peak, about 59 mV. However, the internal reference, ferrocene, which is known to produce a nernstian one-electron wave, gave the same peak potential separation under the same conditions, which is usual for aprotic media where the ohmic drop can be high (∼1 kΩ) without positive feedback. Scan rate studies showed that the anodic and cathodic peak currents (i_{pa}, i_{pc}) of the first oxidation wave were proportional to the square root of the scan rate ($\nu^{1/2}$). Additionally, the peak current ratio (i_{pa}/i_{pc}) was approximately unity down to a scan rate of 50 mV/s, indicating the absence of a following chemical reaction. This suggests that the first oxidation to the stable cation radical is near nernstian for **BH1**−**3**.

The second oxidation wave is only slightly chemically reversible. Taking **BH3** as an example, we could simulate the observed behavior by an EC mechanism, with a homogeneous forward rate constant, $k_f = 10\ s^{-1}$, $K_{eq} = 0.6$, and a heterogeneous rate constant, k_{op}, of about 5×10^{-3} cm^2/s. Figure 2 and Figure 3 show the simulation of both oxidation waves and the reduction side of **BH3** at several scan rates.

The oxidized forms of **BH0** are less stable since they show two sequential chemically quasireversible peaks at 1.64 and 1.83 V. As shown in Table 1, the trend in the potentials for oxidation of

(13) (a) Chandross, E.; Sonntag, F. *J. Am. Chem. Soc.* **1966**, *88*, 1089. (b) Santa Cruz, T. D.; Akins, D. L.; Brike, R. L. *J. Am. Chem. Soc.* **1976**, *98*, 1677.
(14) Ku, S.-Y.; Wong, K.-T.; Bard, A. J. *J. Am. Chem. Soc.* **2008**, *130*, 2392.
(15) Ku, S.-Y.; Chi, L.-C.; Hung, W.-Y.; Yang, S.-W.; Tsai, T.-C.; Wong, K.-T.; Chen, Y.-H.; Wu, C.-I. *J. Mater. Chem.* **2009**, *19*, 773.

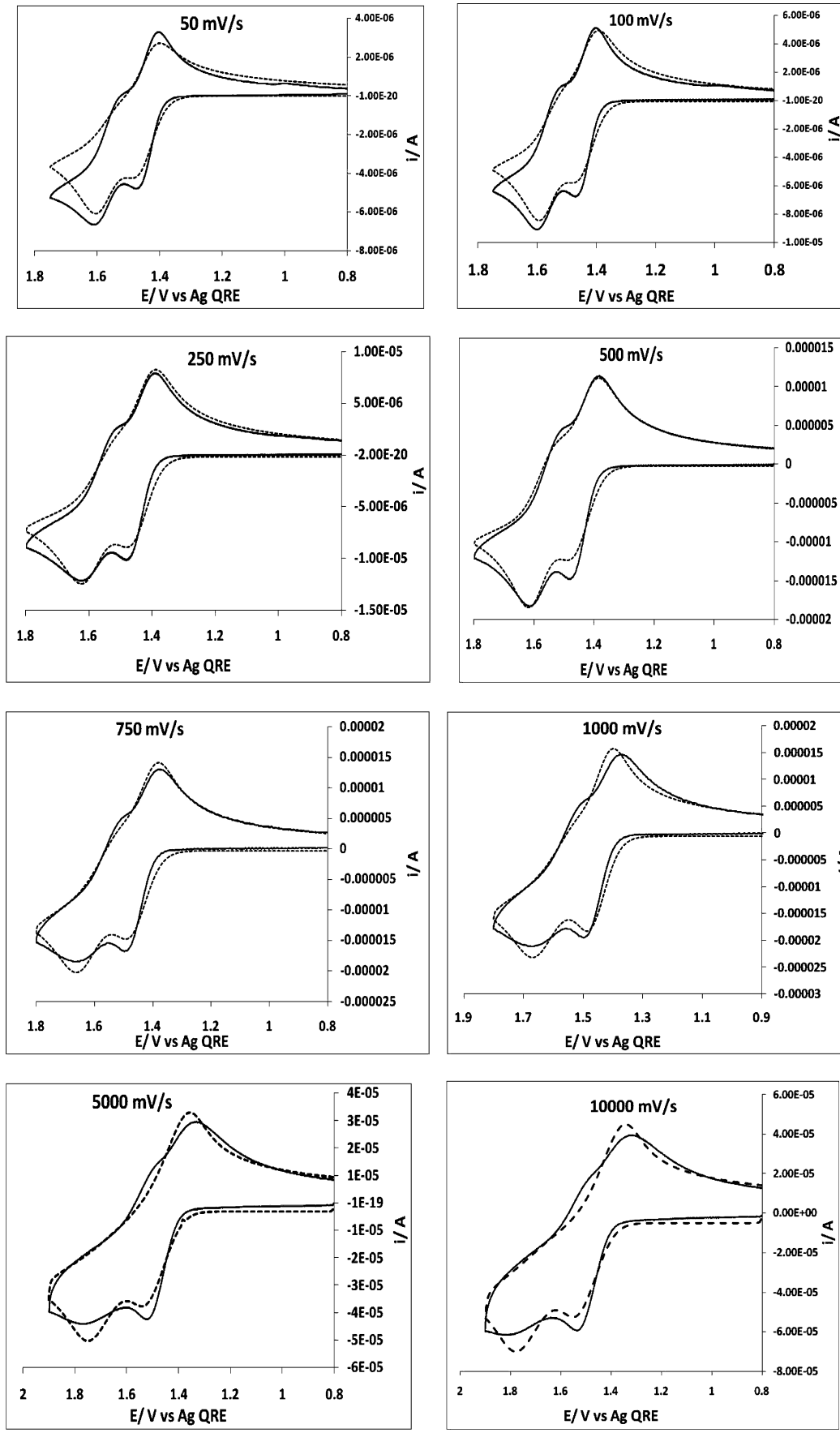

Figure 2. Simulation of oxidation of 1 mM **BH3**. The simulation is corrected for resistance and capacitance: experimental (solid line), simulation (dotted line). The first wave is completely reversible with one-electron transfer ($k_o = 1 \times 10^4$ cm/s), the second wave one-electron transfer of EC mechanism. Ru = 1.2 kΩ, Cd = 10 nF, $\alpha = 0.5$, $D = 9 \times 10^{-6}$ cm^2/s.

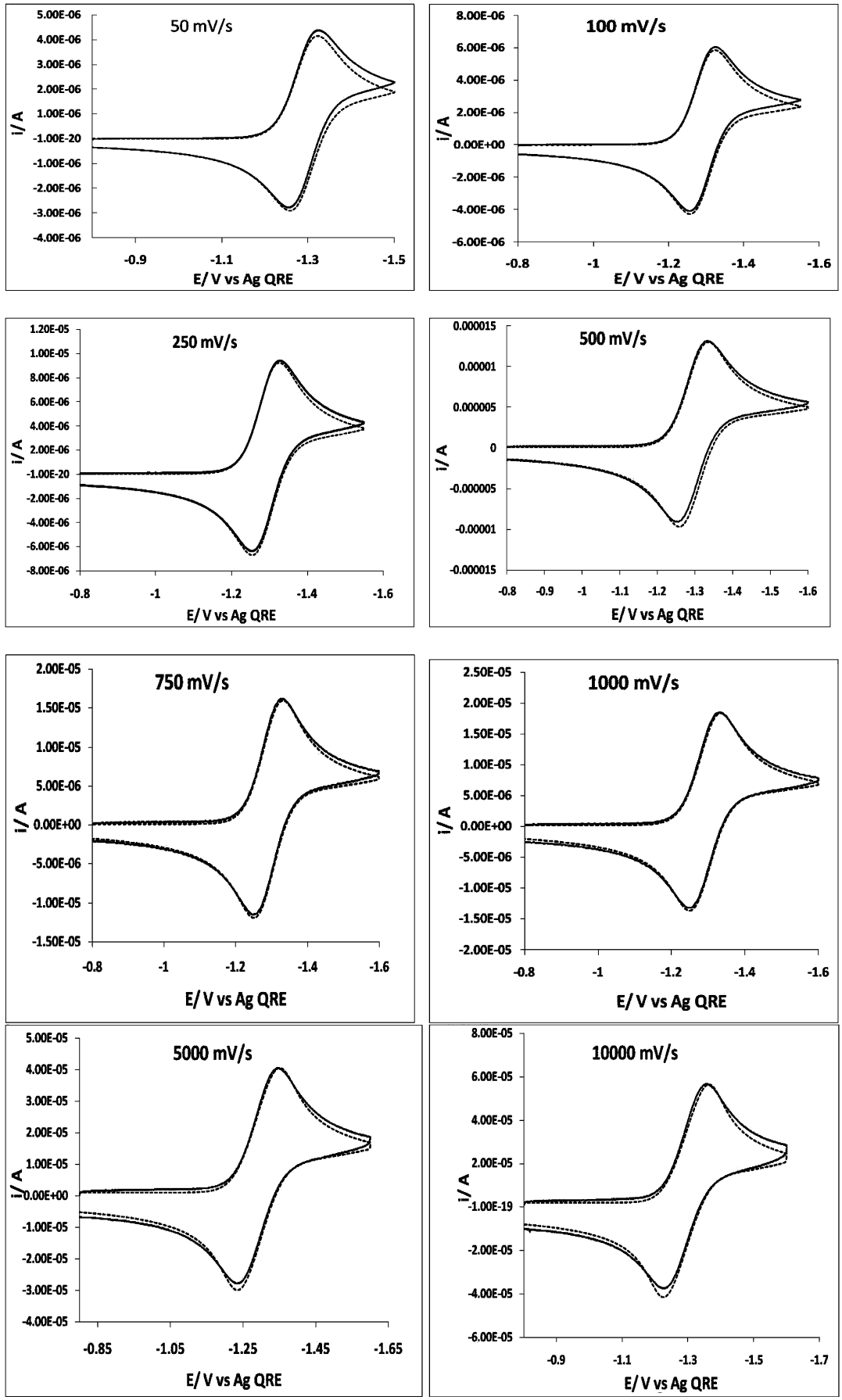

Figure 3. Simulation of reduction of 1 mM **BH3**. The simulation is corrected for resistance and capacitance: experimental (solid line), simulation (dotted line). The reduction is a one-electron transfer process ($k = 1 \times 10^4$ cm/s). Ru = 1.2 kΩ, Cd = 10 nF, $\alpha = 0.5$, $D = 9 \times 10^{-6}$ cm^2/s.

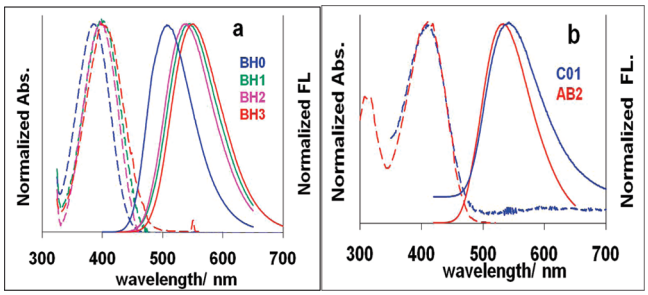

Figure 4. Absorption (dotted lines) and emission (solid lines) spectra. (a) **BH0**−**BH3** in MeCN. (b) **C01** and **AB2** in 1:1 Bz:MeCN. Emission spectra were excited at the absorption maxima.

the first wave is **BH3** < **BH1** < **BH2** < **BH0**. **BH3** with two methoxy groups, which are strong electron donors, is easiest to oxidize followed by **BH1** with one methoxy group. The absence of stabilizing or bulky substituents in **BH0** makes the oxidation more difficult with lesser stability for the radical cation. In fact, because of instability of the cation radical, the wave is shifted to less positive potentials with respect to the thermodynamic $E_{1/2}$, which is thus somewhat more positive than the value shown (Table 1).

BH0 oxidation is distinguishable from that of the other **BHs**. The oxidation waves are less chemically reversible at $\upsilon = 50$ mV/s. Equal anodic peak currents indicate the same number of electrons participate in each oxidation step. However, the first oxidation, which was irreversible at a scan rate $\upsilon = 50$ mV/s, became reversible at $\upsilon > 500$ mV/s, indicating that a homogeneous chemical reaction follows the heterogeneous electron transfer. Simulation of the oxidation wave of **BH0** is shown (Figure S3, Supporting Information). The best fit was an EC mechanism, i.e., a chemical reaction following an electrochemical electron transfer with a heterogeneous rate constant $k_o = 0.025$ cm/s and a homogeneous forward rate constant ($k_f = 3.6$ s^{-1}, $k_{eq} = 0.5$).

Reduction. In scanning negatively, all **BHs** show two reversible reduction waves, as tabulated in Table 1 and shown in Figure 1. A CV of 2,1,3-benzothiadiazole, the central group, taken under the same conditions (Figure S2, Supporting Information), showed a single reversible reduction peak at −1.47 V vs SCE. 2,1,3-Benzothiadiazole is a well-known heteroatomic compound with a high electron-accepting part because it has two electron-withdrawing imine groups (C═N).[16] Thus, this peak for the **BH0** to **BH3** can be attributed to the benzothiadiazole group. The fact that all four compounds show essentially the same potential for reduction demonstrates that there is little effect from the electron-donating substituents.

In addition to the benzothiadiazole peak, all **BHs** show another one-electron reduction peak, which probably corresponds to a second electrochemical reduction of the same benzothiadiazole group for all **BHs** at around −2.18 V vs SCE. The absence of this peak in unsubstituted benzothiadiazole and the presence in the **BH** series might be due to slightly better electron delocalization in the phenyl groups.

Fluorene Derivatives (C01 and AB2). AB2 involves the coupling of two benzothiadiazole groups through a spirobifluorene, while **CO1** involves two spirobifluorenes coupled through a benzothiadiazole group.

Oxidation. A scan toward positive potentials for a **C01** solution shows two sequential reversible waves at 1.46 and 1.61 V vs SCE, respectively (Figure 1). Both have equal peak currents ∼5 μA, consistent with one-electron transfers for the electrochemical oxidation processes. The first peak is chemically reversible down to 50 mV/s, demonstrating a fairly stable cation radical.

The oxidation of **AB2** shows similar behavior as **C01**, with two consecutive, reversible peaks 30 mV less positive than those of **C01** for the first oxidation peaks (1.43 and 1.56 V vs SCE). The small difference is attributed to the greater delocalization in the positive **AB2** cation than the **C01** cation. This delocalization is slightly greater for the **AB2** dication, with a shift of 50 mV compared to the dication of **C01**. These differences imply that the HOMO energy is raised slightly from **C01** to **AB2**.

Reduction. C01 reduction produces two reversible peaks at −1.39 and −1.93 V. Both reductions are expected to occur at the benzothiadiazole group, which is a good acceptor, as discussed previously. Unsubstituted benzothiadiazole does not exhibit a second reduction peak. Here, the second reduction peak of **C01** is less negative than **BH0** by 250 mV. This potential shift indicates greater delocalization onto the two fluorene moieties. In **AB2**, the potential difference is 130 mV because **AB2** possesses only a single fluorene moiety. The first **AB2** reduction peak occurs at −1.44 V and represents a two-electron transfer ($i_{pc} = 10$ μA, compared with $i_{pc} = 5$ μA for the first **C01** reduction and the other peaks), indicating minimal conjugation (electronic communication) through the fluorene moiety so that both benzothiadiazole moieties are reduced at the same potential. However, the second and third reductions of **AB2** show a small splitting of about 150 mV, indicating that in contrast to the dianion radical the benzothiadiazole radical trianion is delocalized across the spirobifluorene moiety. The two processes do not occur at the same potential because the electrostatic repulsion from the second reduction (−2.05 V) shifts the third to more negative potentials (−2.20 V).

Table 2. Spectroscopy Results

	λ_{max}(abs) (nm), [log ε]	λ_{max}(em) (nm)	E_s (eV)[a] 0−0 transition	Φ_{PL} %[b]	Stoke's shifts $\Delta\lambda_{st}$ (nm)
BH0	388,[4.33]	512	2.78	5.0	124
BH1	404,[4.43]	546	2.67	5.5	142
BH2	400,[4.40]	542	2.71	5.2	142
BH3	406,[4.44]	556	2.60	7.0	150
C01	412,[4.61]	544	2.60	90	132
AB2	417,[4.65]	535	2.63	75	118

[a] All spectra recorded in the described solvent at room temperature. Calculated from the wavelength where excitation and emission spectra cross. [b] Quantum yield calculated relative to the fluorescein in solution.

Table 3. ECL Data

compd[a]	λ_{max}^{ECL}/nm	λ_{em}^{FL}/nm	E_s (ev)[b] 0−0 transition	ΔH_{ann}[c]	Φ_{PL} %	Φ_{ECL} %[d]
BH0	518	512	2.78	3.00	2.0	0.05
BH1	560	546	2.67	2.80	4.5	1.40
BH2	556	542	2.71	2.83	4.2	1.35
BH3	555	556	2.60	2.75	5.0	2.35
C01	548	544	2.60	2.87	75	2.7
AB2	536	535	2.63	2.91	65	7.50

[a] All concentrations ∼1 mM. [b] $E_s = hc\,(\tilde{\nu}_{abs} + \tilde{\nu}_{PL})/2$. [c] $-\Delta H = -(E_{pa} - E_{pc}) - 0.1$. [d] Quantum efficiency calculated relative to DPA, assuming DPA is 8%.[18]

Spectroscopy. Absorption and fluorescence spectra for all the compounds are shown in Figure 4. The absorption and emission spectra were obtained in the same solvent mixture used in the electrochemical measurements for the sake of consistency. The optical properties, absorption and emission maxima, extinction coefficient, fluorescence quantum yield, and the optical energy gap are given in Table 2. Structureless $\pi-\pi^*$ absorption bands were observed for fluorene derivatives and **BH0**−**BH3** compounds, suggesting free rotation of the rings in the aromatic system. Compared with **BH0**, **BH1**−**BH3** are red-shifted by 12 nm (**BH2**), 16 nm (**BH1**), and 18 nm (**BH3**), due to electron donor properties of the terminal groups (OMe > propogyl-O > *tert*-butyl). The emission spectra of **BH0**−**3** show the same trend. Compared to **BH0**, **BH1**−**3**, are red-shifted by 30 nm (**BH2**), 34 nm (**BH1**), and 44 nm (**BH3**). **BH0** fluoresces with a $\lambda_{max} = 512$ nm and a Stokes shift of 124 nm, while larger Stokes shifts are observed in **BH1**, **2**, and **3**, as summarized in Table 2.

(16) Yasuda, T.; Imase, T.; Yamamaoto, T. *Macromolecules* **2005**, *38*, 7378.

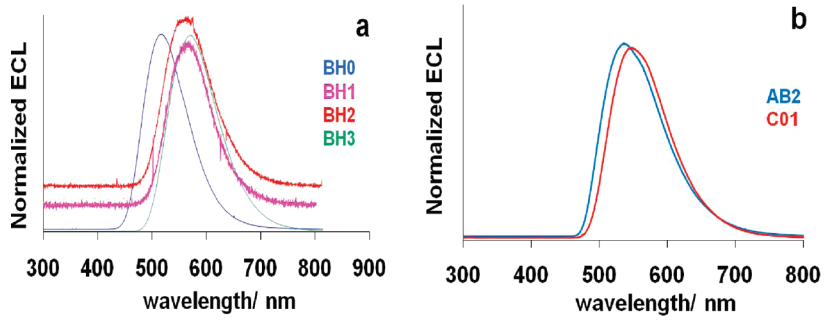

Figure 5. (a) ECL spectra of **BHs** in MeCN, **BH1**, **BH2**, and **BH3** were taken by annihilation by stepping between (E_p^{red} −50 mV) to the first oxidation potential (E_p^{oxd} +50 mV). Integration time, 1 min; slit width, 0.5 mm. **BH0** were recorded using BPO (1 0 mM) as a coreactant. (b) ECL of fluorene derivatives by annihilation by stepping between (E_p^{red} −50 mV) to the first oxidation potential (E_p^{oxd} +50 mV).

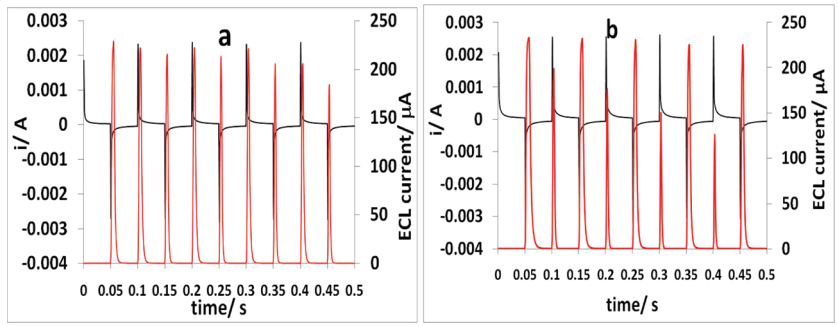

Figure 6. Stepping ECL (annihilation) of **BH3** (1 mM), in MeCN. Pulse width, 0.05 s; stepping direction is from anodic to cathodic. (a) From the first oxidation peak (1.35 V) ($n \sim 1$) to the first reduction peak (−1.50 V) ($n = 1$). (b) From both oxidation peaks (1.50 V) ($n = 2$) to the first reduction peak (−1.50 V) ($n = 1$), pulse width = 0.05 s. (As plotted here, the positive electrochemical current is the anodic pulse, and the negative electrochemical current is the cathodic pulse.)

The absorption λ_{max} for **AB2** and **C01** are slightly red-shifted because of their greater conjugation. There is a slightly smaller Stokes shifts for **AB2** and **C01** compared to the **BHs**, which could be due to the smaller solvent polarity used for these compounds, Bz:MeCN, compared to pure MeCN in the case of **BHs**.

Electrogenerated Chemiluminescence (ECL). All **BHs** and the fluorene derivatives produced strong ECL emission for radical ion annihilation, which can be seen with the naked eye in a dimly lit room; typical results are given in Table 3 and Figure 5. In all cases, the estimated annihilation energy is sufficient to populate the excited singlet state directly, classifying the ECL of these systems as energy sufficient or S-route systems. All ECL spectra were close to the PL spectra; the 5−15 nm difference between the PL and ECL is probably caused by instrumental differences and the self-absorption (inner filter effect) from the high concentrations of the solutions used for ECL vs those for PL studies.

BH0 produced only weak ECL by direct annihilation (sweeping or stepping potentials between the first oxidation and reduction peaks). This results from instability of the radical cation, as seen in the oxidative cyclic voltammogram. Because of this instability of the **BH0** radical cation, the ECL intensity decreased with time, and a spectrum could not be obtained with the liquid nitrogen cooled CCD camera as a detector during extended pulsing. However, in this case, a coreactant approach could be used. Since the radical anion of **BH0** is stable, BPO was used as a coreactant for reductive ECL. BPO, upon reducing electrochemically, produces a strong oxidizing agent (E^{oxd} = 1.5 V vs SCE),[13,1a] which can react with the radical anion of **BH0** populating the excited state. Under these conditions, strong ECL was observed (Figure 5a).

To estimate the stability of the ECL and the radical ion species involved, potential pulsing ECL transients were collected. For example **BH3** shows two consecutive oxidation waves and one reduction peak (one-electron transfers). When the potential was stepped from the first oxidation wave ($E_{pa,1}$ +50 mV) to the reduction wave ($E_{pc,1}$ −50 mV), approximately equal ECL peaks were observed on the cathodic and anodic pulses, consistent with the same quantities of radical anions and cations formed per pulse and stability of the radical ions during the time of the experiment (Figure 6a). When the potential was stepped to the second oxidation wave ($E_{pa,2}$ +50 mV) producing the dication A^{2+}, the anodic current was smaller than the cathodic current and the ECL maximum intensities were about the same as for pulsing to the first oxidation wave (Figure 6b). However, the decay rate of the anodic ECL transients is higher (Figure 6b). Moreover, the ECL intensity of the anodic pulse decreased with time, while in the cathodic, ECL intensity was constant. There have not been many studies of ECL generation between radical anions and dications, and the situation is complicated because of the occurrence of a comproportionation reaction between the dication and parent and also by the fact that all of the electrogenerated species are potential quenchers. Although we have tried to simulate the observed behavior by choosing different rate constants for the possible reactions, we were not successful in matching the observed experimental results. Interpreting these kinds of asymmetric ECL generation will probably be easier in a steady state (two-electrode) mode, e.g., by scanning electrochemical microscopy (SECM).

The relative quantum efficiencies were determined for all the ECL emitters, as calculated by the number of photons emitted per injected electron. These were compared to 9,10-diphenylanthracene (DPA) as a standard ECL emitter, even though the emission (λ_{max} = 420 nm) is quite blue-shifted compared to the compounds of interest here. These results are given in Table 4, taking the quantum yield of DPA in acetonitrile as 8%.[13] The ECL emission intensity of **AB2** is about the same as that of DPA but in the green region of the spectrum.

Conclusions

We have synthesized a series of highly fluorescent and strong, green ECL emitters. These compounds were characterized by electrochemistry, spectroscopy, and thermal analysis. All the compounds, with the exception of **BH0**, give reversible oxidation and reduction waves in their CV and form stable radical ions. Due to their high PL quantum yield

and stable radicals upon electrooxidizng and reducing, these gave strong and stable green ECL emission. The ECL quantum yield of **AB2** is close to that of the well-known ECL emitter, DPA. Such fluorene derivatives are promising for future applications as nanomaterials and biological luminescent labels.

Acknowledgment. We thank the National Science Foundation (CHE 0451494 and 0808927), Roche BioVeris, and the Robert A. Welch Foundation (F-0021) for support of this research, Dipankar Koley for assistance with the digital simulation of the ECL experiments, and the financial support from the National Science Council of Taiwan.

Supporting Information Available: Details of characterization of the compounds and additional experimental results. This material is available free of charge via the Internet at http://pubs.acs.org.

JA904135Y

(17) Gritzner, G.; Kuta, J. *Pure Appl. Chem.* **1984**, *56*, 462.

(18) Beideman, F. E.; Hercules, M. *J. Am. Chem. Soc.* **1979**, *83*, 2203.